

Practical Applications of Coherent Transition Radiation

Michael J. Moran

University of California,

UCRL--96936

Lawrence Livermore National Laboratory

DE88 002574

P.O. Box 808, L-45

Livermore, CA, 94550 USA

The predictable nature of transition radiation (TR) emissions has been demonstrated under a wide variety of experimental conditions. The reliable character of TR allows the design of specific practical applications that use emissions from the optical to the x-ray spectral regions. Applications often can be enhanced by the spatial coherence of TR, and some have become highly developed. New applications may be developed through the use of other related radiation mechanisms.

DISCLAIMER

This report was prepared as an account of work sponsored by an agency of the United States Government. Neither the United States Government nor any agency thereof, nor any of their employees, makes any warranty, express or implied, or assumes any legal liability or responsibility for the accuracy, completeness, or usefulness of any information, apparatus, product, or process disclosed, or represents that its use would not infringe privately owned rights. Reference herein to any specific commercial product, process, or service by trade name, trademark, manufacturer, or otherwise does not necessarily constitute or imply its endorsement, recommendation, or favoring by the United States Government or any agency thereof. The views and opinions of authors expressed herein do not necessarily state or reflect those of the United States Government or any agency thereof.

MASTER

DISTRIBUTION OF THIS DOCUMENT IS UNLIMITED

When a relativistic charged particle crosses a dielectric boundary transition radiation (TR) is emitted into forward and backward (or reflected) narrow cones.^{1,2,3} TR has value for a wide range of applications because the radiation is extremely broad band (from below the visible to above x-ray energies) and is a relatively efficient photon source, even for particle speeds that are only mildly relativistic. Examples of applications range from coherent optical TR in electron beam diagnostics to the design of high-flux x-ray sources.^{4,5,6,7}

These applications often can be enhanced in a predictable fashion by exploiting the inherent spatial coherence of TR. For example, the emission distributions from multi-foil radiators display interference patterns that can be highly sensitive to experimental parameters such as the electron beam energy or emittance.⁴ These interference effects have been described accurately by simplified versions of the theory of TR under a wide variety of experimental conditions.^{4,5,8}

The reliable character of TR distributions allows the design of highly specific experiments. This predictability and the basic nature of TR can be understood in terms of three simple concepts: the "virtual photons" associated with charges in motion,⁹ the idea of a "formation length" for photon emission, and the Lorentz contraction and Doppler shift commonly associated with relativistic processes. Because of their usefulness for understanding TR phenomena (and, incidentally, numerous other radiation mechanisms), these concepts will be described briefly below.

The "virtual photon" spectrum of an energetic charged particle is the Fourier spectrum of the coulomb field of the charge. That is, virtual photons represent the frequency content of the time-dependent coulomb field associated with a charge as it passes by some given point of "measurement". The virtual photon spectrum of a moving charge can be written as:⁹

$$dN/d\omega \approx (\alpha/\pi\omega)\ln(A\gamma), \quad (1)$$

where N is the number of photons, ω is the photon angular frequency, α is the fine structure

constant ($\alpha = 1/137$), γ is the relativistic energy parameter ($\gamma = (\text{total energy})/(\text{rest mass})$), and A is a constant of order unity. This distribution has a low intensity (because of the factor of α), but has constant energy density for all photon energies up to the particle kinetic energy (where it is artificially terminated). Further study of the virtual photon distribution reveals that photons with frequency ω will be "found" within a transverse distance b_ω of the charge, where b_ω is given by $b_\omega = \gamma\lambda/2\pi$ (where λ is the photon wavelength). Virtual photons can be said to have transverse spatial coherence over distances of order b_ω .

The second concept, the "formation length" is a measure of the distance that a charge must travel in order to radiate a photon by some given mechanism. For TR, the formation length also may be thought of as the distance over which a charge travels while an accompanying photon travels a distance which differs by one-half wavelength (see Fig. 1). For a charge traveling through a medium with dielectric constant $\epsilon(\omega)$ and refractive index $n(\omega) = \sqrt{\epsilon(\omega)}$, and with relativistic speed $\beta = \sqrt{1-1/\gamma^2}$, the formation length Z may be written as:

$$Z = (\lambda/2)/(1-1/n\beta). \quad (2)$$

For relativistic particle energies, this formula often gives formation lengths that are decades greater than the wavelength of interest. These long formation lengths indicate a delicate and predictable phase relationship between the charge and a radiated photon, because the photon emission takes place over relatively long distances. This precise phase relationship is the basis of the spatial (longitudinal) coherence properties of TR.

The two concepts described above can be used to give a fairly complete picture of TR emission distributions. The formation length is simply the minimum amount of material required at an interface in order for efficient emission to occur: the emission occurs as the charge travels one formation length into the new medium. The phase of the emitted photon is spatially correlated to the positions of both the interface and the charge. As the charge crosses an

interface, it radiates its entire virtual photon spectrum (at least for those frequencies for which there is a formation length of material at the interface). Thus, the spectral density of virtual photons in Eq. (1) is nearly identical to angle-integrated formulas for single-interface TR spectral densities.¹⁰

The form of TR angular distributions can be explained by symmetry arguments and by the transverse coherence of virtual photons. The dielectric boundary presents a longitudinal perturbation to the moving charge. Since longitudinal perturbations of motion tend to generate radiation patterns with "zeros" in the longitudinal direction, TR can be expected to have an on-axis minima in its angular distributions. Furthermore, since the photons are radiated with transverse coherence distances of order b_ω , the photons can be expected to be radiated into a cone with angular width $\Delta\theta \sim \lambda/(2b_\omega)$. Substitution of the form given above for b_ω gives a cone angle $\Delta\theta \sim 1/\gamma$ (within factors of π), independent of frequency. For TR, the arguments above correctly suggest that the angular distribution would be a "hollow" cone with a half-angle of $1/\gamma$.

The third concept that describes the behavior of relativistic radiation processes is the severe contraction of characteristic lengths of the radiating system. The contraction can be severe because it consists of the Lorentz contraction with a subsequent Doppler shift. The net effect of these contractions is to give a wavelength $\lambda \sim L/2\gamma^2$ in the forward direction. For photons emitted at an angle θ , a better description of the contracted wavelength is given by:

$$\lambda = (L/2\gamma^2)(1 + \gamma^2\theta^2)$$

(3)

The factor of γ^2 means that, with relativistic charged particles, macroscopic periodic structures can be designed to coherently radiate photons with microscopic wavelengths. For example, with 50 MeV electrons, structures with cm spacings will tend to radiate photons with sub- μm (optical) wavelengths. As long as the particle's motion is not severely disturbed, the

spatial coherence that is established at each radiating element (or interface) will be maintained as the particle passes through the entire structure. Thus, the electric field amplitudes radiated by the entire structure can add coherently. This behavior leads to interference effects whereby the emission distributions from multi-element radiators are drastically altered, compared to those from a single interface.^{4,5,8} This effect is apparent even for the photons generated at the two surfaces of a single foil.¹¹

The concepts described above can be used to design experiments with TR that address a wide variety of practical applications. The design for particular applications can be expressed in terms of three basic experimental components: the incident electron beam, the foil target or radiator structure, and the radiated photon beam, with associated diagnostics (see Fig. 2). If any two of these components are well understood, then the experiment can be used to study some aspect of the third.

For example, if the system includes a two-foil radiator (where the foils are transparent and have a known complex dielectric constant) and well-characterized diagnostics to measure optical TR, then the system can be used to diagnose relativistic electron beams. This is perhaps the most fully developed application of TR.^{4,5} Optical TR systems have been designed that can measure the electron beam transverse profile, the beam energy, and the emittance of beams with energies from 20 to 100 MeV. The biggest disadvantages of this technique are that the foils may represent a significant disturbance to the electron beam and that the foils may not survive in high-current electron beams. At the same time, this technique is highly efficient in terms of the quantity and quality of data that can be retrieved in an experiment. This is especially true of the emittance data, which is extremely difficult to obtain with conventional techniques.

The beam emittance can be determined accurately from the interference patterns that result when TR from two spatially separated surfaces are superimposed in an appropriate manner.⁵ Here, the spatial and angular distributions of the electron beam affect the character of the recorded interference patterns. Calculations then can be used to model the system and infer

the beam emittance by matching the TR interference patterns.

A different set of applications become available when a known electron beam is incident on multiple-foil radiators, where the electron beam energy and foil parameters are chosen so that the system acts as an efficient photon source. One application that our own experiments have explored is to use electron beams with energies in the 25- to 100-MeV range and multiple-foil radiators as an intense soft x-ray source. The simplest sources of this type generate bands of soft x rays (with \approx 50% bandwidth) with energies in the 0.1- to 5.0-keV regions.¹² The band of x-ray energies radiated by the source can be "tuned" with choice of foil thicknesses and electron beam energy. These sources often can be fairly efficient, generating tens of joules of x rays per coulomb of incident electrons. With nominal operation of the LLNL linac, sources of this type have generated 3 mW c.w. of soft x rays, with peak powers exceeding 300W (because of the short pulses generated by the accelerator). Under these conditions, we have succeeded in demonstrating soft x-ray lithography¹³, and have measured single x-ray pulses with relatively insensitive high-bandwidth x-ray detectors. Sources of this type can be advantageous for a variety of experimental situations.

Another type of application arises when the experiment includes a known incident electron beam and well-characterized diagnostics for measuring emitted radiation, with some aspect of the radiating target remaining to be specified. In this case, the experiment can be used to study different characteristics of the target. The emitted radiation distributions are sensitive to both the dielectric constants (or photon scattering cross sections) of the target material, as well as gross structural features of the material. For low-density foams, data already has been published demonstrating that TR spectra can be interpreted in terms of the foam cell diameter and cell wall thickness.¹⁴ Our own experiments have recorded similar preliminary data for low-density reticulated structures. Here, the spectra and angular distributions reflect the "strut" diameter and typical separation for the particular material.

In a similar fashion, the TR interference patterns from multi-foil radiators and spectrally-resolved diagnostics can be used to infer frequency-dependent dielectric constants of

materials in the x-ray spectral region.^{15,16} Data of this type can complement similar data being recorded at synchrotron facilities with different techniques. The advantage of this technique is that absolute photon intensities need not be measured, as the dielectric constants are inferred from the qualitative angular distributions. This technique represents a direct measurement of $\epsilon(\omega)$, and the data can be very specific in multiple-foil radiators where the interference patterns become highly distinctive.

Further development of the applications mentioned above go hand in hand with improvements in electron beam technology: as the quality of beams improves, the applications can become more specific and better defined. For these situations, improved beam quality means lower emittance or reduced beam divergence for given beam diameters. TR can contribute to these improvements by providing specific and well defined diagnostics.

For transition x-ray sources, improved electron beams would allow the development of narrow-band tuneable sources. Our experiments have demonstrated the feasibility of this technology. These sources consist of closely spaced multiple-foil radiators whose emission distributions are strongly affected by interference effects. Figure 3 shows an example of the emission distribution from one such source. The source consists of a target with 6 0.5- μm thick boron nitride (B_5N) foils exposed to a beam of 100-MeV electrons. The energies of the emitted x rays correlate with the angles of emission; and, for a given angle of emission, the x-ray spectral width can be less than 10%. Changing the selected angle of emission can be used to select the desired x-ray energy (lower x-ray energies are emitted at larger angles). The output can be tuned further by varying the incident electron energy. Sources of this type could address the spectral region from 0.1 to 5 keV, using electron energies from 25 to 150 MeV.

One of the most exciting directions for new developments in this area of technology is with other closely-related radiation mechanisms. To see this, note that the concepts of virtual photons, formation lengths, and relativistic contraction describe not only TR, but also can be applied to a large number of other radiation mechanisms, including Cherenkov radiation,¹⁷

bremsstrahlung, synchrotron radiation, diffraction radiation, and channeling radiation.

Following the TR examples, further applications using these other radiation mechanisms may be feasible, although the required electron energies or radiated photon energies may be different.

The range of conceivable applications include such ideas as solid-state short-wavelength FEL's,^{18,19,20} or intense, coherent γ -ray sources, or coherent x-ray sources capable of holographic imaging of biological microstructures. In view of the exciting nature of some of the possible applications, research with TR and coherent photon generation mechanisms in general might have a bright future indeed.

This work was performed at the Lawrence Livermore National Laboratory under the auspices of the U.S. Department of Energy under Contract No. W-7405-Eng-48.

REFERENCES

- ¹V.L. Ginzburg and I.M. Frank, J. Phys. (Moscow) 9, 353 (1945).
- ²M.L. Ter-Mikaelian, "High Energy Electromagnetic Processes in Condensed Media" (Wiley-Interscience, New York, 1972).
- ³R.H. Ritchie and H.B. Eldridge, Phys. Rev. 126, 1935 (1962); and A.L. Frank, E.T. Arakawa, and R.D. Birkhoff, Phys. Rev. 126, 1947 (1962).
- ⁴L. Wartski, S. Roland, J. Lasalle, M. Bolore, , and G. Filippi, J. Appl. Phys. 46, 3644 (1975).
- ⁵D. Rule, Nucl. Inst. and Meth. in Phys. Res. B24/25, 901 (1986).
- ⁶M.A. Piestrup, J.O. Kephart, H. Park, R.K. Klein, R.H. Pantell, P.J. Ebert, M.J. Moran, B.A. Dahling, and B.L. Berman, Phys. Rev. A32, 917 (1985).
- ⁷M.J. Moran and P.J. Ebert, Nucl. Inst. and Meth. in Phys. Res. A242, 355 (1986).
- ⁸M.J. Moran, B.A. Dahling, P.J. Ebert, M.A. Piestrup, B.L. Berman, and J.O. Kephart, Phys. Rev. Lett. 57, 1223 (1986).
- ⁹W.K.H. Panofsky and M. Phillips, "Classical Electricity and Magnetism" (Addison-Wesley, Reading, Mass., 1962), p. 352.
- ¹⁰M.L. Cherry, G. Hartman, D. Muller, and T.A. Prince, Phys. Rev. D10, 3594 (1974).
- ¹¹P.J. Ebert, M.J. Moran, B.A. Dahling, B.L. Berman, M.A. Piestrup, J.O.Kephart, H. Park, R. K. Klein, and R.H. Pantell, Phys. Rev. Lett. 54, 893, (1985).
- ¹²A.N. Chu, M.A. Piestrup, P.F. Finman, R.H. Pantell, and R.A. Gearhart, IEEE Trans. Nucl. Sci. NS-29, 336 (1982)) and P.F. Finman, M.A. Piestrup, R.H. Pantell, and R.A. Gearhart, *ibid.* p. 340.
- ¹³M.A. Piestrup, M.J. Moran, B.L. Berman, P. Pianetta, and D. Seligson, Proc. SPIE 773, p. 37 (Proc. Conf. Electron- Beam, X Ray, Ion-Beam Lithography, Santa Clara, CA, March, 1987).
- ¹⁴M.L. Cherry, Phys. Rev. D17, 2245 (1978).
- ¹⁵X. Artru, G.B. Yodh, and G. Mennessier, Phys. Rev. D12, 1289 (1975).
- ¹⁶M.J. Moran, B.A. Dahling, M.A. Piestrup, B.L. Berman, and J.O. Kephart, Proc. Conf on X Rays in Materials Analysis, San Diego, CA, Aug. 1986, Proc. SPIE 690, p. 146.

- 17 M.J. Moran, B. Chang, M. Schneider (to be published).
- 18 M.A. Piestrup and P.F. Finman, IEEE J. Quant. Elect. QE-19, 357 (1983).
- 19 J.E. Walsh, Phys. of Fluids, 20, 709 (1977).
- 20 G. Kuriski, M. Strauss, J. Oreg, and N. Rostoker, Phys. Rev. A35, 3424 (1987).

FIGURE CAPTIONS:

Figure 1 Here, the formation length Z is described in terms of different path lengths traveled by an electron and a co-propagating photon. During time τ the electron travels distance Z , while the photon travels a distance D that is greater by one-half wavelength. During this time, energy transfer can occur between the two different particles.

Figure 2 A TR experiment can be described in terms of three basic components: the electron beam, the target or radiator, and the radiated photon beam with associated diagnostics. Accurate specification of any two of the components allows the experiment to study some aspect of the third component.

Figure 3 This contour plot shows the angular dispersion of x-ray energies for a specific set of experimental conditions. The intensity contours are plotted with increments of .015 photons/elect.-ster.-eV. The contours are analogous to Fabry-Perot optical fringes. For any continuous contour lower x-ray energies are radiated at larger angles. For any given angle, energy definition is better than 10%.

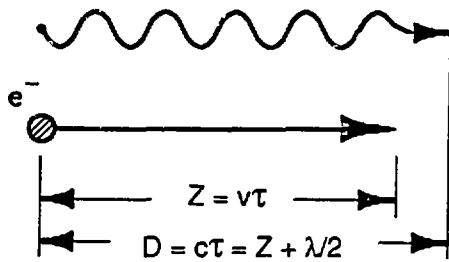


FIGURE 1

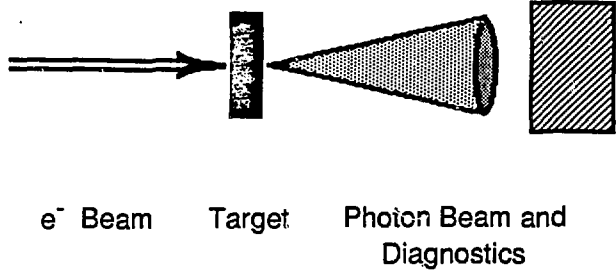


FIGURE 2

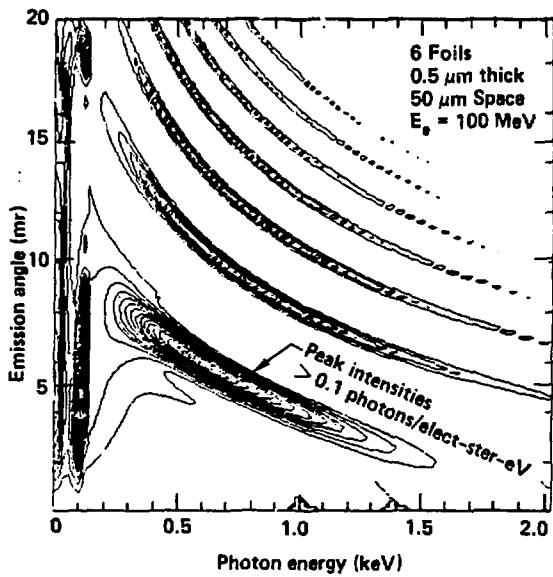


FIGURE 3